

Fine particle retention and deposition in regions of cyclonic tidal current rotation



M.E. Williams^{a,b,*}, L.O. Amoudry^a, J.M. Brown^a, C.E.L. Thompson^c

^a National Oceanography Centre, Liverpool, UK

^b Departamento de Obras Civiles, Universidad Técnica Federico Santa María, Valparaíso, Chile

^c School of Ocean and Earth Science, University of Southampton, Southampton, UK

ARTICLE INFO

Editor: Edward Anthony

Keywords:

Tidal benthic boundary layer

Fine sediment

Mud retention

Cyclonic tidal currents

Mud deposit

ABSTRACT

Benthic sediments in continental shelf seas control a variety of biogeochemical processes, yet their composition, especially that of fine sediment, remains difficult to predict. Mechanisms for mud or fine sediment deposition and retention are not fully understood. Using sediment data and a hydrodynamic model of the Northwest European shelf seas, a relationship is shown to exist between fine benthic sediment composition and regions of cyclonic tidal current rotation. The reduced thickness of cyclonic tidal benthic boundary layers compared with the anticyclonic case promotes deposition of fine sediment and trapping of resuspended material. Adding the effects of the benthic boundary layer thickness, as influenced by ellipticity or not, sheds some light on the limitations of approaches only focusing on bed shear stress and sediment pathways to predict the location of mud deposits. A tidal boundary layer predictor that includes ellipticity alongside tidal current magnitude and depth was shown to spatially agree with maps of mud deposits.

1. Introduction

Coastal and shelf seas cover a small fraction of the ocean but are of utmost importance and value (e.g. Costanza et al., 1997). Sediments in these regions act as valuable resources and support the majority of global benthic biogeochemical cycling of organic matter (Jørgensen, 1983). Sediment composition (mud, sand, gravel) influences a range of biogeochemical and physical parameters. Biogeochemical processes depend on sediment type, varying between advective sediments (sand, gravel) with low organic content and cohesive sediments (mud) with high organic content (Somerfield et al., 2018). Sediment type influences physical processes in shelf seas through modification of bed friction (van Rijn, 2007), thus impacting dissipation of energy, and sediment mobility (Hsiao and Shemdin, 1980; Soulsby, 1997; Winterwerp and van Kesteren, 2004). It also influences benthic habitats and community structure (e.g. Rees et al., 1999; Sharples et al., 2013; Somerfield et al., 2018). Understanding the overall structure and functioning of shelf seas, including their response to human and climate pressures, thus requires an understanding of sediment composition, transport, and deposition mechanisms.

While sand and gravel benthic sea floor composition in shelf seas is relatively predictable with bed shear stress controlling their distribution (e.g. Ward et al., 2015), mechanisms of mud dispersal and

retention are still not fully understood (Macquaker et al., 2010). Recent work has illuminated the influence of high energy episodic events to mud deposit shape and location, and to the movement of mud on and off of the continental shelf. Zhang et al. (2016) showed storm waves on the Iberian shelf resuspended fine sediment that was redistributed by a transient oceanic frontal current. Cheriton et al. (2014) observed internal waves on the California coast suspended fine sediment from the shelf slope which traveled in nephroid layers to feed a mud deposit on the Monterey Bay shelf. Internal waves and tides are likely an important mechanism for sediment transport on all continental slopes (Boegman and Stastna, 2019). Anthropogenic influences on mud deposits also exist. Trawling is capable of inducing gravity flows near steep topography to move mud from the shelf edge to deeper regions (Payo-Payo et al., 2017). Episodic events have been shown to dominate mud transport on narrow shelves (Harris and Wiberg, 1997) and across longer timescales, repeated episodic events cause transport of fine sediment across a shelf (e.g. Moriarty et al., 2015). For broad shelves, ocean tides can also generate large currents and tidal processes are important. For example, tidal resuspension is frequent in the Celtic Sea (Thompson et al., 2017b). Low bed shear stress and sediment-transporting residual flows are typically considered to be the hydrodynamic processes required for fine sediment deposition and retention in such systems (e.g. Zhou et al., 2015). Shelf sea circulation provides pathways

* Corresponding author at: Departamento de Obras Civiles, Universidad Técnica Federico Santa María, Valparaíso, Chile.

E-mail address: megan.williams@usm.cl (M.E. Williams).

<https://doi.org/10.1016/j.margeo.2019.01.006>

Received 20 July 2018; Received in revised form 14 January 2019; Accepted 16 January 2019

Available online 19 January 2019

0025-3227/ © 2019 The Authors. Published by Elsevier B.V. This is an open access article under the CC BY license (<http://creativecommons.org/licenses/by/4.0/>).

for fine sediment movement, and convergence of these residual currents can create regions of high fine sediment concentration (McCave, 1972), while tidal resuspension can be frequent (e.g. Thompson et al., 2017b).

Despite the study of mud deposits on many shelves, the capability to predict mud deposit location and spatial extent is limited. Ward et al. (2015) successfully predicted coarse sediment composition in the Irish Sea and Celtic Sea using numerically modeled bed shear stresses and bed samples. However, they under predicted sediment grain size in a Celtic Sea region of low bed shear stress and over predicted it in the eastern Irish Sea where bed shear stress is not very low but a mud deposit is present. Other authors have turned to machine learning and spatial statistics to predict benthic sediment composition (Stephens and Diesing, 2015; Wilson et al., 2018; Bockelmann et al., 2018). In the Northwest European shelf seas, Stephens and Diesing (2015) found mud was present where the shelf seas were more than 50 m deep. Wave orbital velocities become smaller with depth, so wave-generated bed shear stresses increase with shallower water. The implication is a spatial gradient in mud resuspension, whereby mud can be resuspended at shallower depths and moved to deeper depths where it is less likely to be resuspended. Moriarty et al. (2015) observed this trend on the Waipaoa Shelf of New Zealand.

Sediment transport in shelf seas is closely linked to circulation and depends on erosion and deposition, processes which are all dependent on boundary layer dynamics. The water column in a shelf sea has a surface and benthic boundary layer. The surface boundary layer is generated by wind and waves, while the benthic boundary layer is generated by the oscillatory flow due to tides (and surface waves if shallow enough) over a rough bed. Differences in these controls lead to differences in benthic boundary layer thickness. Wave boundary layers are typically limited in height to a few centimeters (e.g., Grant and Madsen, 1986) but are important to sediment transport due to their relatively high sediment concentration, sometimes resulting in sediment gravity flows (e.g. Zhang et al., 2016). In comparison, tidal benthic boundary layers reach tens of meters and can also drive large sediment flows. Boundary layers are regions of enhanced turbulence and are important in a range of bio-physical processes - including controlling scalar fluxes into sediments or resuspension via periodic turbulence (Lorke et al., 2003; Soulsby, 1983) and influencing phytoplankton transport to benthic organisms (Fréchette et al., 1989). In shelf seas where tidal currents are elliptical, the direction of current rotation also influences the benthic boundary layer thickness (Soulsby, 1983). Prandle (1982) showed with an analytical solution that depending on latitude, tidal benthic boundary layers could not fully develop when rotating counter to the Coriolis force because the timescale to fully develop the flow is longer than the tidal period. Simpson and Tinker (2009) made measurements at two locations in the Celtic Sea with opposite rotation to confirm Prandle's prediction. This thinner boundary layer has been suggested to influence retention of cohesive muds in the *Nephrops norvegicus* fishing grounds in the Celtic Sea (Sharples et al., 2013). If this is the case, retention of pollutants such as microplastics west of Ireland (Martin et al., 2017) and radioactive sediments in the eastern Irish Sea (Kershaw et al., 1988) would also be influenced by the rotational direction of tidal currents. We present the hypothesis that the suppressed boundary layer in cyclonic tidal currents aids the deposition and retention of fine sediment, and is an important mechanism to consider in shelf sediment dynamics, and therefore of pollutant, carbon, or nutrient retention.

Using model data we examine the relationship between tidal current polarity and muddy benthic sediment, demonstrating that high mud concentration sediment on the Northwest European shelf are found only where currents are cyclonic. We demonstrate that this pattern cannot be replicated considering only bed shear stress, depth, and a sediment pathway. We then explain the physical processes responsible for the relationship between fine sediment and cyclonic tidal currents. By applying a boundary layer predictor which accounts for ellipticity (also sometimes referred to as polarity or eccentricity, Davies, 1985; Simpson

and Tinker, 2009) and scaling it by depth we create a metric to show where rotational effects will influence boundary layer dynamics (and thus benthic sediment composition). Then, by reversing the ellipticity in the predictor, we observe which mud deposits might not exist in their current form if not for the direction of tidal currents, and which are influenced by rotational effects in the presence of low bed shear stress and/or deep water.

This manuscript presents a background to continental shelf sediments and hydrodynamics, including boundary layer effects of cyclonic tidal currents. The relationship between ellipticity and muddy sediment on the shelf is presented, focusing on four regions of the Northwest European shelf and the shelf in general. We show that depth and bed shear stress alone cannot account for the distribution of muds. The physical controls on the ellipticity - mud relationship are explored through the boundary layer effects, and then the relevance is depicted with a parameterization of the boundary layer thickness normalized by depth.

2. Background on tidal boundary layers in shelf seas

Currents on continental shelf seas are primarily driven by tides and the effect of Earth's rotation (Soulsby, 1983). Prandle (1982) analytically derived a tidal current profile in the presence of the Coriolis force, showing that the prevalence of tidal rotation with Coriolis (anticyclonic/*con sole*) or against Coriolis (cyclonic/*contra solem*) influences the height of the tidal benthic boundary layer. This benthic boundary layer is on the order of tens of meters, and regardless of the tidal current rotation is much larger than the wave boundary layer that extends tens of centimeters, if not less (e.g. Grant and Madsen, 1986).

Horizontal tidal currents (U , V) can be considered in the sinusoidal form,

$$U = a_u \cos(\omega t) + b_u \sin(\omega t) \quad (1)$$

and

$$V = a_v \cos(\omega t) + b_v \sin(\omega t) \quad (2)$$

where a and b are the amplitudes of the currents, ω is the tidal frequency, and t is time.

Combining Eqs. (1) and (2) into the vector form, $\mathbf{R} = U + iV$ allows the tidal currents to be split into clockwise and counterclockwise rotating currents, since the formula for any tidal ellipse can be given by the sum of a positive and a negative rotating circular current (see, e.g. Defant, 1961),

$$\mathbf{R} = \mathbf{R}_+ + \mathbf{R}_- \quad (3)$$

with the rotational components equal to

$$\mathbf{R}_+ = \frac{1}{2}[(a_u + b_v) + i(a_v - b_u)]e^{i\omega t} \quad (4)$$

$$\mathbf{R}_- = \frac{1}{2}[(a_u - b_v) + i(a_v + b_u)]e^{-i\omega t} \quad (5)$$

Using this division into rotating components, Prandle (1982) defined the boundary layer thickness (δ) of the positive component to be

$$\delta_+ = \frac{cu_*}{\omega + f} \quad (6)$$

and the negative component to be

$$\delta_- = \frac{cu_*}{\omega - f} \quad (7)$$

where c is a constant, u_* the shear velocity, and f the Coriolis parameter.

In the Northern Hemisphere where $\omega > f$ (below 74°N for the M_2 tide) and f is positive, δ_+ is small compared to δ_- . In the Southern Hemisphere the opposite is the case (Fig. 1a).

Since elliptical tidal currents can be defined as the sum of the positive and negative rotating circular currents, the composite tidal

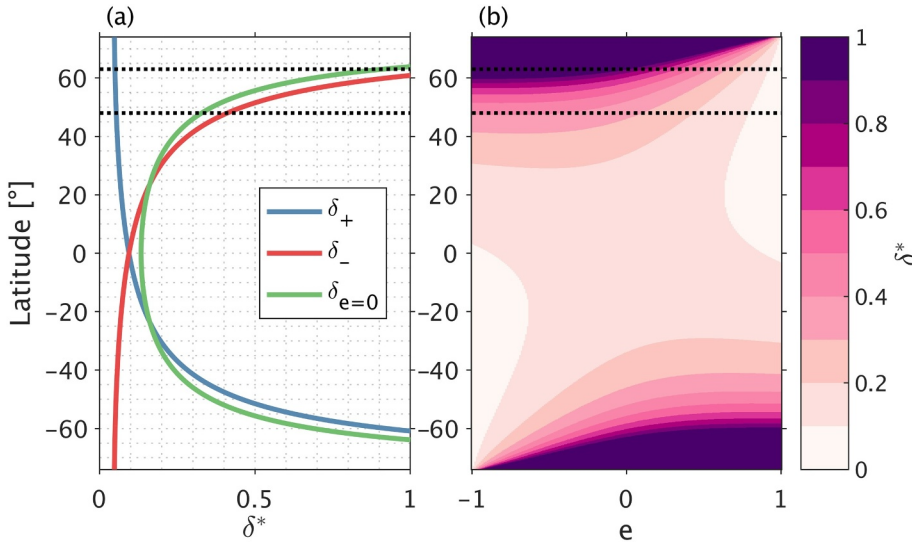


Fig. 1. (a) The boundary layer for positive and negative rotating tidal currents across latitudes for M_2 tides. (b) Variation of the scaled boundary layer thickness for latitude and ellipticity. Black dotted lines give the limits of the shelf seas in Fig. 2. Values plotted in Eq. (11) are $c = 0.075$, $C_D = 0.0025$, $U_{rms} = 0.75 \text{ ms}^{-1}$, and $H = 75 \text{ m}$.

boundary layer in the presence of the Coriolis force is given by the scaled

$$\delta = \frac{|\mathbf{R}_+|}{|\mathbf{R}_+| + |\mathbf{R}_-|} \delta_+ + \frac{|\mathbf{R}_-|}{|\mathbf{R}_+| + |\mathbf{R}_-|} \delta_- \quad (8)$$

Soulsby (1983) then used the definitions $R_+ = U_a + U_b$ and $R_- = U_a - U_b$, and the parameterization $u_* = C_D^{1/2} u$ (where C_D is a drag coefficient) to define the boundary layer thickness as

$$\delta = \frac{c C_D^{1/2}}{2} \left[\frac{U_a \omega - U_b f}{\omega^2 - f^2} \right] \quad (9)$$

By defining the ellipticity,

$$e = \frac{U_b}{U_a} \quad (10)$$

where U_b is negative for clockwise rotating currents, and normalizing by depth (H), the non-dimensional boundary layer thickness, δ^* , is

$$\delta^* \equiv \frac{\delta}{H} = \frac{c C_D^{1/2}}{2H} \left[\frac{U_a (\omega - ef)}{\omega^2 - f^2} \right] \quad (11)$$

As $e \rightarrow \pm 1$, Eq. (11) goes to $\frac{\delta_+}{H}$ or $\frac{\delta_-}{H}$.

To estimate boundary layer thickness on the Northwest European shelf, Soulsby (1983) used a depth-averaged tidal model and found $c = 0.075$ based on measurements by Pingree and Griffiths (1977). Using these values, and for $U_{rms} = 0.75 \text{ ms}^{-1}$ and $H = 75 \text{ m}$, and $C_D = 0.0025$, the structure of the boundary layer as modified by cyclonic tidal current rotation is clear (Fig. 1b). Values of u_* , c , and C_D given in Soulsby (1983) show that the height of the benthic boundary layer in a cyclonic tidal current is reduced compared to a rectilinear boundary layer, and in the anticyclonic case the limit on boundary layer height is controlled by the water depth or stratification, not rotational effects. Observations by Simpson and Tinker (2009) in the Celtic Sea showed that where $e = 0.6$ the benthic boundary layer was limited to 20 m above the bed while at $e = -0.6$ the boundary layer extended to 70 m above the bed, the height of the pycnocline.

3. Methods

3.1. The Northwest European shelf

The Northwest European shelf seas consist of the North Sea, Irish Sea, Celtic Sea, English Channel, and the shelf west of Ireland and Great Britain (Fig. 2). The shelf seas have an M_2 dominant tide and are generally less than 200 m deep (Fig. 2b), with much of the shelf only

submerged after the 120–135 m eustatic sea level rise of the last deglaciation (Clark and Mix, 2002). Sand and gravel dominate benthic sediment composition, but mud deposits of varying geographic extent are found in the Irish Sea, Celtic Sea, west of Ireland, and in the North Sea (Fig. 2a). Many of these mud deposits are commercially important fishing grounds for *Nephrops norvegicus* (commonly known as Norwegian lobster, langoustine, or scampi). Mud deposits in the northern North Sea (Fladen and Witch Grounds) are of early Holocene origin (Jansen, 1976; Jansen et al., 1979), perhaps forming during different hydrodynamic conditions of a lower sea level or as a deglaciation effect. The western Irish Sea mud belt is present under a seasonal baroclinic gyre (Hill et al., 1994). In the eastern Irish Sea, the mud patch remains depositional as evidenced by radioactive sediments from nearby Sellafield, a nuclear decommissioning site on the west coast of Northern England whose nuclear materials history dates to the 1950s (Kershaw et al., 1988).

3.2. Sediment data

We obtained the distribution pattern of benthic sediments around the United Kingdom from the British Geological Survey (BGS) DIGSBS250 dataset. These data are given as polygons of sediments classified by a Folk 15 triangle (Folk, 1954) plus bedrock, diamicton, and two mixed sediment types. A Marine Institute of Ireland dataset uses a Folk 7 classification of six sediment types plus bedrock to collate and standardize data from various sources, including those which have been ground-truthed and those relying on VMS data from fishing vessels, and an assumption of the relationship between *N. norvegicus* habitat and mud content (e.g. Bell et al., 2013).

For analysis, we consider here gravels to be sediment with composition > 30% gravel (mG, msG, sG, and G in the Folk 15 triangle), sands to be < 30% gravel and with a ratio greater than 1:1 in the sand to mud ratio (mS, S, (g)mS, (g)S, gmS, and gS in the Folk 15 triangle), and muds to be < 30% gravel and less than 1:1 sand to mud (M, sM, (g)M, (g)sM, and gM in the Folk 15 triangle) (Fig. 4). High mud percentage sediment is considered here to have a < 1:9 sand to mud ratio and be < 5% gravel, corresponding to mud (M) and slightly gravelly mud ((g)M) in the Folk 15 triangle, which are both classified as mud in the Folk 7 triangle. Marine Institute Folk 7 data are included here in maps (Fig. 2a), but not in the comparison of ellipticity to bed sediment type because the data are a compilation with varying levels of confidence and some patchy spatial coverage.

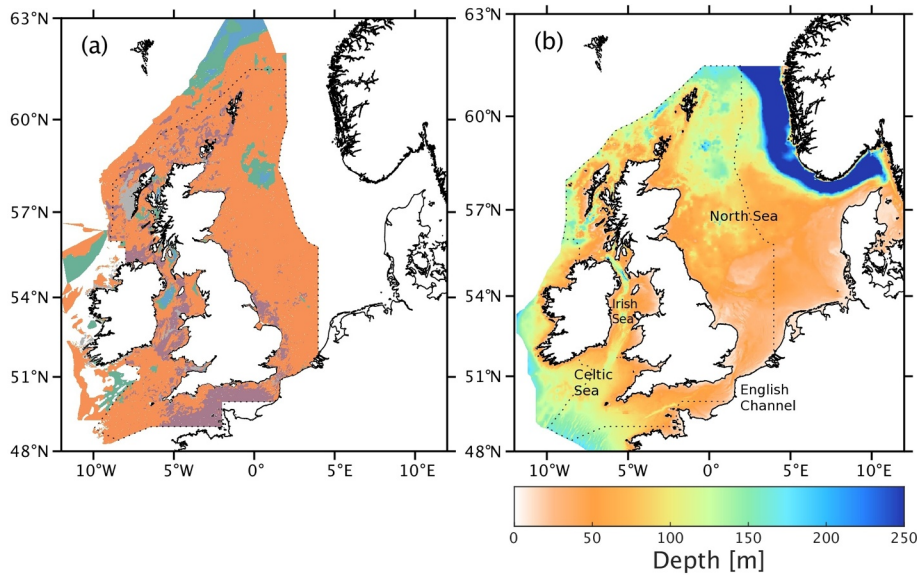


Fig. 2. (a) Regions of muds (blues), sands (orange), gravels (purple), and other sediments (grey) from the BGS DigSBS250 dataset of UK waters and mud (blues) and sand (orange) regions from Marine Institute data. Colors correspond to those outlined on the Folk triangle (Fig. 4). Regions in grey are coarser sediments to bedrock while white indicates no data. (b) Bathymetry of the shelf seas. The black dotted line shows the area of overlap of hydrodynamic model grid and BGS sediment classification data. (For interpretation of the references to color in this figure legend, the reader is referred to the web version of this article.)

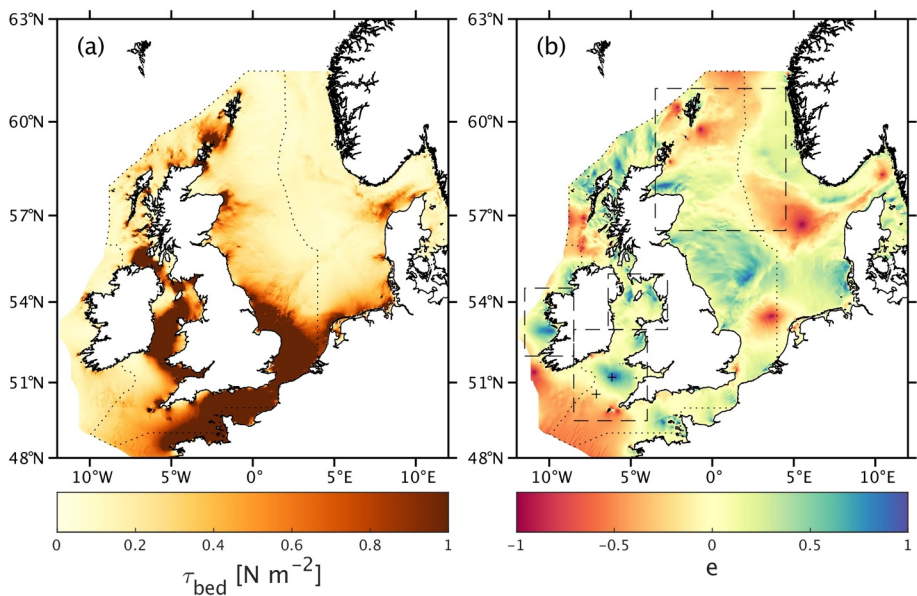


Fig. 3. (a) The calculated 90% exceedance bed shear stress over the Northwest European shelf. (b) Near-bed M_2 tidal ellipticity, e . Positive ellipticity (yellow to blue) in the Northern Hemisphere corresponds to cyclonic current rotation and negative ellipticity (orange to red) currents are anticyclonic. Regions of muddy sediment explored in further detail are outlined in dashed lines and virtual mooring locations (+) in Fig. 8 are in the southern most rectangle. The black dotted line shows the area of overlap of hydrodynamic model grid and BGS sediment classification data. (For interpretation of the references to color in this figure legend, the reader is referred to the web version of this article.)

3.3. Numerical ocean model

To examine the physical controls on benthic sediment composition at the shelf scale, hydrodynamic characteristics, such as bed shear stress (Fig. 3a) and ellipticity (Fig. 3b), are obtained from ocean model outputs. We use the Proudman Oceanographic Laboratory Coastal Ocean Modelling System (POLCOMS, Holt and James, 2001), which was developed to model the dynamics of the Northwest European shelf and has been extensively validated for that purpose (e.g., Holt et al., 2005; Holt and Proctor, 2008; O'Neill et al., 2012). The three-dimensional baroclinic hydrodynamic model is coupled to the General Ocean Turbulence Model (GOTM, Umlauf et al., 2005) to model ocean turbulence (Holt and Umlauf, 2008) and to the shallow water version (Monbaliu et al., 2000) of the WAVE Model (WAM, Komen et al., 1994). The overall modeling system is applied to the whole Northwest European shelf at high resolution (~ 1.8 km in the horizontal and 32 vertical σ layers, Holt and Proctor, 2008) and simulations were conducted for a full calendar year (2008) to integrate over seasonal timescales (Brown et al., 2015a, 2016). One-way nesting within an Atlantic Margin Model provided offshore boundary conditions for water elevation, currents,

temperature and salinity. The Atlantic Margin Model is in turn forced from the Met Office Forecast Ocean Assimilation Model (FOAM, Bell et al., 2000) and tidal forcing consists of 9 constituents (e.g. Holt et al., 2005). Atmospheric forcing for the high-resolution shelf model provided hourly wind velocity and atmospheric pressure, along with three-hourly cloud cover, relative humidity and air temperature. The model bathymetry was taken from the Northwest European shelf Operational Oceanographic System (NOOS, Holt and Proctor, 2008) with a minimum depth of 10 m applied to prevent stability problems caused by wetting and drying on the coast.

Residual currents, bed shear stresses, and values of turbulence parameters are calculated from a baroclinic simulation coupled to the wave model. Bed shear stresses are obtained from the near-bed velocity assuming a near-bed logarithmic layer. Analysis of model data for bed shear stress gives 90% exceedance values. These values are computed at each spatial point where they are the 90% intercept of the cumulative distribution of time-varying stress over the full year. Ellipticity is calculated from a tide-only simulation, which was found to agree with results from the baroclinic simulation with waves and therefore used to focus on tidal processes. Values show good agreement with ADCP

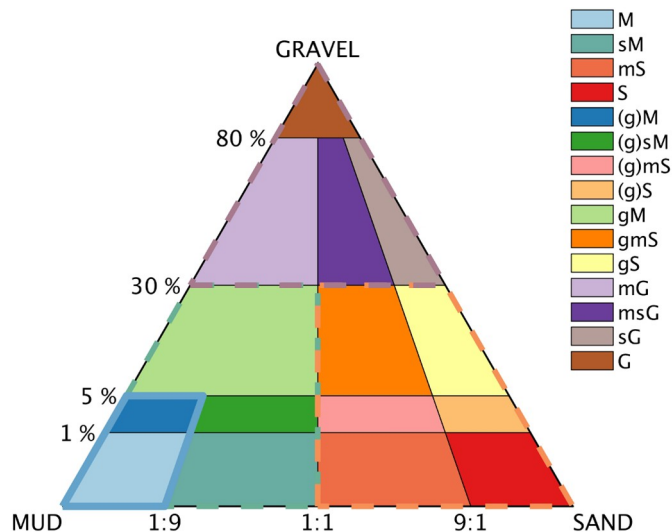


Fig. 4. The modified Folk diagram used in BGS data (Folk, 1954). The high mud content classifications (M and (g)M) are outlined in blue. Gravels, sands, and muds depicted in Fig. 2 are outlined in the corresponding color. (For interpretation of the references to color in this figure legend, the reader is referred to the web version of this article.)

measurements made in the Celtic Sea for a different year (Thompson et al., 2017a). To maintain consistency with Soulsby (1983), ellipticity is calculated from the depth-averaged M_2 tidal current component using tidal harmonic analysis (Pawlowicz et al., 2002). To calculate U_a in Eq. (11), depth-averaged currents (again for consistency with Soulsby, 1983) were rotated into principle flow direction and the largest rotated current was defined as U_a . In this way the boundary layer height was determined by all tidal constituent currents, not just the M_2 currents, even though they dominate on the shelf and determine here the rotational direction. To match sediment spatial polygon data and gridded hydrodynamic model data, the grid points located within each sediment polygon type were selected to compare sediment, stress, ellipticity, and

bathymetry data. The domain where sediment and model data are compared is shown with dotted lines on the maps in Figs. 2 and 3.

4. Results

Numerical model results for the Northwest European shelf seas show that the M_2 ellipticity across the shelf is often positive at locations with benthic mud deposits (Figs. 2a, 3b). West of Ireland, in the Celtic Sea, and in the northern Irish Sea, regions where ellipticity is highly positive are present, and in the northern North Sea M_2 ellipticity is slightly positive where a large mud deposit is present (dashed boxes on Fig. 3b). Bed shear stress varies across the shelf (Fig. 3a). High bed shear stress regions have been shown to correspond to coarse sediments (Ward et al., 2015, Fig. 3a). High bed shear stresses are primarily due to tidal velocities, though wave stresses are high in some regions, e.g. on the southeast English coast (Neill et al., 2010). Some regional lows match the locations of mud deposits, but low bed shear stress and mud distribution do not generally have the same spatial pattern (Figs. 2a, 3a).

The M_2 ellipticity at each grid point within a BGS sediment classification reveals muds are rarely found where ellipticity is negative (Fig. 5). Looking at all the sediment types shows the tidal ellipticity in the shelf seas is more likely to be positive than negative, as shown by the histogram of all data points (Fig. 5g). Gravels are found where ellipticity is positive and negative (Fig. 5e, f). Sands are similarly found where ellipticity is both positive and negative (Fig. 5c, d). The distribution of muddy sediment, however, is skewed toward positive ellipticity, with nearly the entire distribution of high mud concentration data points located in shelf locations where ellipticity is positive (Fig. 5a, b).

The histograms normalized by all sediment types show that the sand fraction dominates the Northwest European shelf. The mud percentage of the shelf sediments is small compared to sand, but with a clear bias toward positive ellipticity (Fig. 5b). Near $e = 0$ a dip in the sand fraction exists with a rise in the gravel fraction (Fig. 5d, f). Rectilinear flow has $e = 0$, so these correspond to areas of high bed shear stress in narrow channels and inlets.

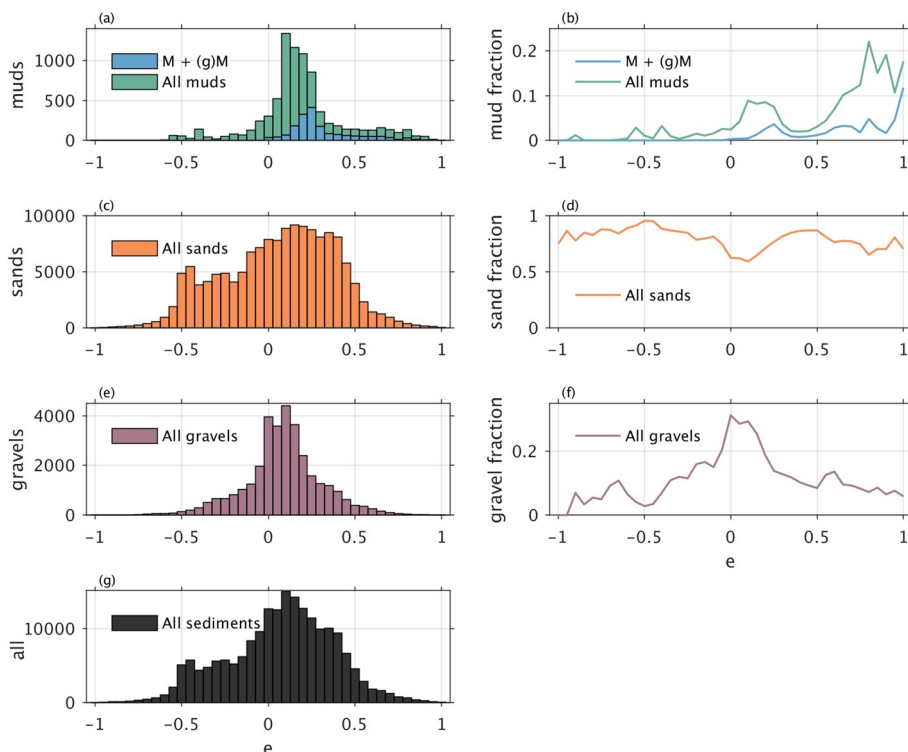


Fig. 5. The distribution of each sediment classification within the range of bed ellipticity values. (a) Muds ($< 1:1$ sand:mud and $< 30\%$ gravel) in green and the high mud corner of the Folk triangle ($< 1:9$ sand:mud and $< 30\%$ gravel) in blue, (b) the mud fraction across the domain, (c) sands ($> 1:1$ sand:mud and $< 30\%$ gravel), (d) the sand fraction across the domain, (e) gravels ($> 30\%$ gravel), (f) the gravel fraction across the domain, and (g) the distribution across all sediments (including sediments that do not fall within the Folk triangle). Across the shelf, positive ellipticity dominates, but few muds and almost no high mud % sediment locations are located within regions of negative ellipticity. (For interpretation of the references to color in this figure legend, the reader is referred to the web version of this article.)

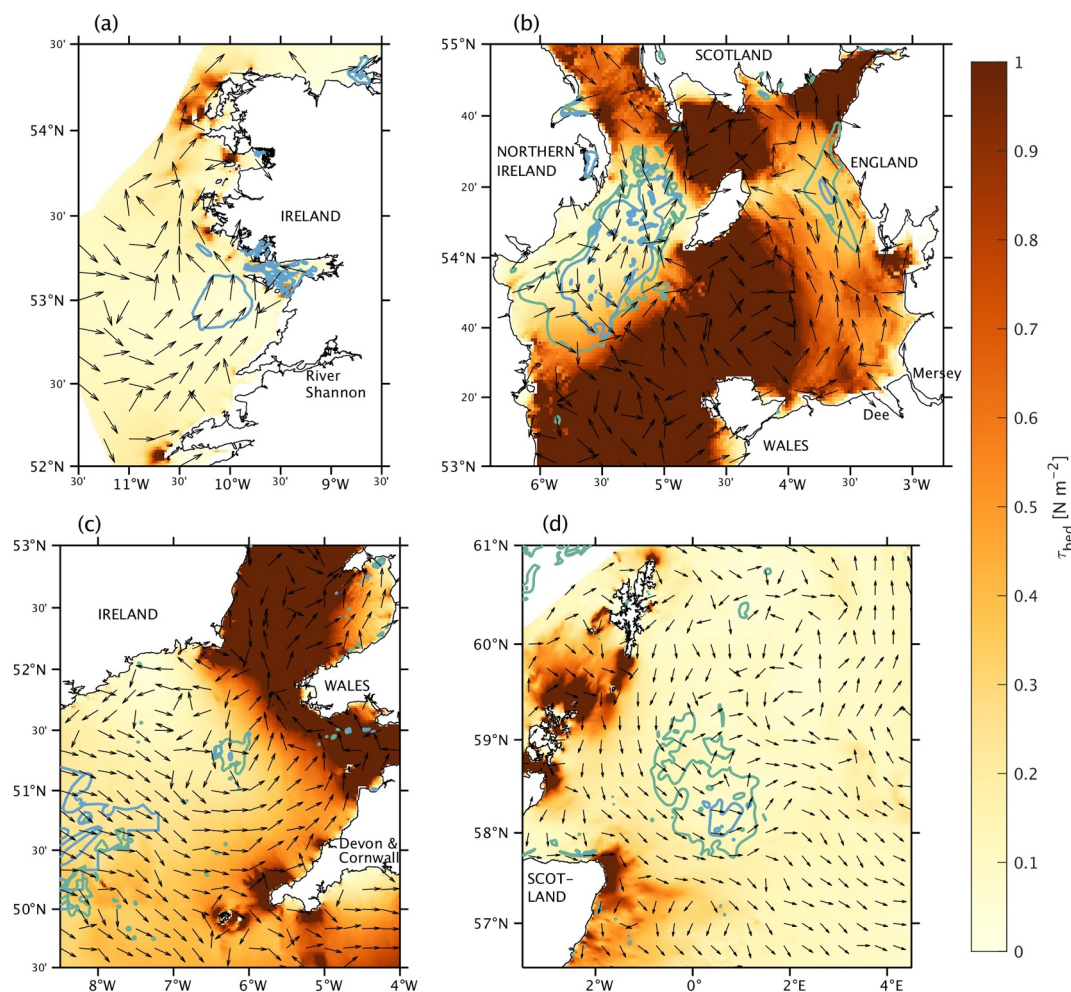


Fig. 6. Bed shear stress 90% exceedance with the surface residual velocity direction overlain in arrows for four locations on the Northwest European shelf. Sediments from the mud corner of the Folk 15 triangle are outlined in green while high mud percentage (M + (g)M) sediment is outlined in blue. (a) West of Ireland, (b) the northern Irish Sea, (c) the Celtic Sea, and (d) the northern North Sea. (For interpretation of the references to color in this figure legend, the reader is referred to the web version of this article.)

4.1. Focus on regional examples

Much of the Northwest European shelf seas have positive ellipticity (Figs. 3b, 5g), so we investigate other processes relevant to fine sediment transport and deposition to question whether the observed relationship between ellipticity and mud is important. Here we focus on bed shear stress and on residual flows. Fig. 6 shows bed shear stress in four regions overlain with the direction of the residual surface currents and outlines of fine sediment deposits.

4.1.1. Aran Grounds (Atlantic Ocean)

In the Atlantic Ocean west of Ireland (Figs. 2a, 6a), the Aran Grounds *N. norvegicus* fishery is located in a large mud patch (centered around 10° W, 53° N). Bed shear stresses are low across the entire area, not only where muds are present. Surface residual currents show northward flow of the Irish coastal current. Fine particles carried in the residual current are likely sourced from the River Shannon, which drains the largest watershed in Ireland (Cullen and McCarthy, 2003). No convergence of a surface residual exists and there is little spatial variability of bed shear stress to explain the fine sediment spatial heterogeneity.

4.1.2. Northern Irish Sea

In the northern Irish Sea, two mud deposits are present (Figs. 2a, 6b). Spatial variability of bed shear stress here agrees with the presence

of both the western and eastern mud deposits. In the eastern Irish Sea, the spatial distribution of low bed shear stress matches that of muddy sediment such that bed shear stresses are lowest where muds are found. Fine particles from estuaries (e.g. the Dee and the Mersey) are transported northward by surface residual currents as demonstrated by a particle tracking modeling study (Brown et al., 2015b). Here, the residual transport and low bed shear stress may qualitatively explain the presence of finer sediment without needing to consider the rotation of tidal currents. However, Ward et al. (2015) over-predicted the sediment grain size in this region, suggesting that the magnitude of bed shear stress, though locally low, may not be small enough to quantitatively explain the presence of muds.

In the western part of the northern Irish Sea, modeled bed shear stresses show low values exist where muds are present in the Western Irish Sea mud belt. Spatial agreement exists between our numerical model and that of Ward et al. (2015), and in this region Ward et al. (2015) was more successful here than in the eastern part of the northern Irish Sea in reproducing the spatial distribution of the fine sediment deposit. The residual flow directions are highly varied (see arrows in Fig. 6b), with evidence of surface currents from the north and from the Irish coast, with some circulation apparent over the deposit. Here, a seasonal baroclinic gyre is present, and has been identified as a retention mechanism over this mud deposit (Hill et al., 1996, 1994).

4.1.3. Celtic Sea

In the Celtic Sea, mud is present in a patch centered around 6.25° W, 51.25° N (Figs. 2a, 6c). The Marine Institute dataset shows mud farther out (southwest) on the shelf, but the BGS dataset only gives a few small mud patches there, so the focus here is the more northerly mud deposit. Bed shear stresses are low across a large region of the Celtic Sea extending from the mud patch to the coast of Ireland (Fig. 6c), and hydrodynamic modeling efforts erroneously predict dominance of fine particles across this entire region (Ward et al., 2015). The River Severn feeds into the Bristol Channel (between Wales and Devon and Cornwall) and drains a large watershed through a muddy estuary, making it a potential source of fine sediment to the Celtic Sea mud deposit. Residual currents exhibit complex spatial structure. Nevertheless, mud pathways inferred here by residual surface currents can be distinguished not only between the Bristol Channel and the mud patch (first moving north along the Welsh coast then south over the muddy region), but also to and from the southeast coast of Ireland (Fig. 6c). The surface residual velocity arrows show some indication of a retentive gyre around the mud patch in the Celtic Sea here and in previous measurements, which may influence sediment retention (Brown et al., 2003). Overall, this suggests that additional processes help constrain the mud patch to its confined location.

4.1.4. Northern North Sea

A large mud deposit is located in the northern North Sea (Figs. 2a, 6d). Similar to west of Ireland, low bed shear stress regions extend much beyond the mud deposit. The early Holocene nature of these mud deposits suggests that locating a sediment source and pathway may not be relevant here if this mud deposit is no longer active, though the Dooley current (Holt and Proctor, 2008) is visible in the residual flow over the mud deposit. Slightly north of the mud and sandy mud, some convergence of surface residuals occurs, but not in the region of the finest benthic sediments. The known early Holocene origin of this mud deposit poses the question, why has mud remained in distributed patches within this region?

4.2. Shelfwide

The regional focus demonstrated the spatial variability of bed shear stress in locations with mud deposits. Here we present a comparison of depth and bed shear stress with ellipticity for all data points within our domain.

Depth and bed shear stress are not independent variables as high stresses are more likely found at shallow depths and low stresses in deep waters, but we examine both variables across sediment type here to compare to benthic sediment predictions (e.g. Stephens and Diesing, 2015). Comparing M + (g)M to all sediments shows that muds are found across a range of depths on the Northwest European shelf, though are largely absent shallower than 50 m (Fig. 7a), in general agreement with the depth limit for muds found by Stephens and Diesing (2015) for the Northwest European shelf seas. Data points near the 10 m limit are found in the Bristol Channel where high sediment supply and estuarine processes coexist, along the Belgian Coast, and in shallow areas of the Western Scottish Islands. The cluster of points between 30 and 40 m depth and e between 0.54 and 0.64 are found in the eastern Irish Sea mud deposit. Other values shallower than 50 m are found on the edge of the western Irish Sea mud path, and in coastal areas within the islands of Scotland.

Bed shear stress values show considerably less agreement with predictions for muddy sediment (Fig. 7b). Muddy sediment is not found at very high bed shear stress, but are also found above what Thompson et al. (2017b) predicted for shelf muddy sediment critical erosion threshold (ranges shown in the blue rectangle, Fig. 7b). Points near $e = 0$ at the highest bed shear stress are those shallow locations described in the preceding paragraph. The points within the eastern Irish Sea mud deposit are visible above other bed shear stress values between

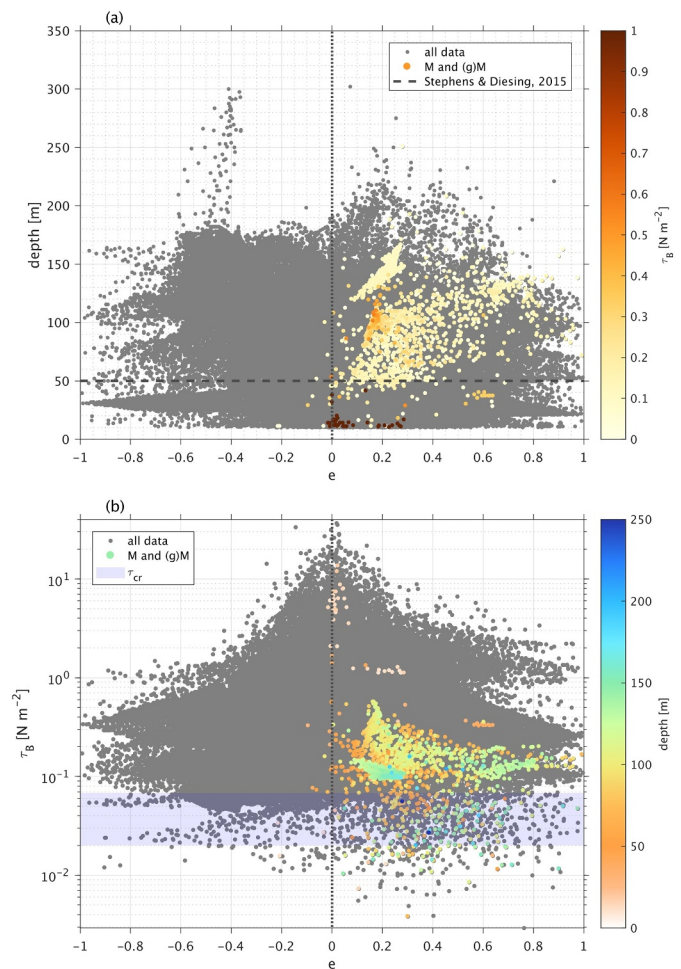


Fig. 7. (a) M_2 tidal ellipticity and bathymetry for all points with the mud points overlain and scaled by bed shear stress. 50 m depth is indicated, corresponding to the Stephens and Diesing (2015) limit where muds are found. (b) M_2 tidal ellipticity and bed shear stress for all grid points contained within a BGS polygon with the mud points overlain and scaled by bathymetry. The blue shading gives the range of critical erosion stress measured in situ at a muddy site at 103 m depth in the Celtic Sea (Thompson et al., 2017a). $e = 0$ is indicated in both plots. (For interpretation of the references to color in this figure legend, the reader is referred to the web version of this article.)

$e = 0.54$ to 0.64 . The shelf-wide data shows that bed shear stress and depth dependencies are not sufficient to explain fine sediment distribution on the continental shelf since bed shear stress is in most locations above the critical erosion threshold.

4.3. Benthic boundary layer thickness

Numerical model results for the turbulent boundary layer at two locations with cyclonic and anticyclonic currents confirm the analytical prediction that cyclonic tidal currents have a suppressed cyclonic boundary layer compared to the anticyclonic case. Fig. 8 gives turbulent diffusivity (K_z) at two locations in the Celtic Sea (indicated by (+) on Fig. 3b), with ellipticity either strongly positive ($e = 0.86$, cyclonic) or weakly negative ($e = -0.10$, anticyclonic). K_z is used here to define the boundary layer thickness relevant to fine sediment because sediment diffusivity is commonly assumed to be the same as turbulent diffusivity (Amoudry and Souza, 2011), and results are shown for the month of June 2008 to focus on a time period where the surface and benthic boundary layers are decoupled in the absence of strong winter storms. The cyclonic benthic boundary layer is seen oscillating on a spring-neap cycle from less than 20 m above the bed to almost 35 m

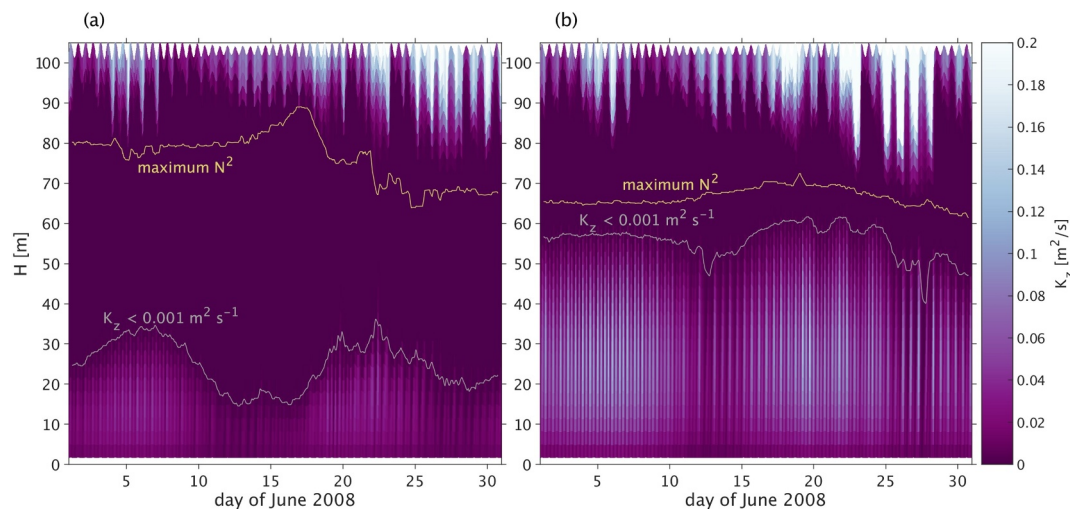


Fig. 8. Vertical structure at the modeled locations in the Celtic Sea for June 2008. (a) K_z where $e = 0.86$ and (b) K_z where $e = -0.10$. The grey line shows boundary layer thickness defined as where K_z falls below $10^{-3} \text{ m}^2 \text{ s}^{-1}$. The yellow line gives the location of maximum $N^2 = -\frac{g}{\rho_0} \frac{\partial \rho}{\partial z}$ to show stratification. The cyclonic (positive ellipticity) boundary layer thickness is limited by rotation counter to the Coriolis force while the anticyclonic (negative ellipticity) boundary layer thickness extends to the pycnocline. (For interpretation of the references to color in this figure legend, the reader is referred to the web version of this article.)

above the bed (shown as the height above the bed where K_z falls below $10^{-3} \text{ m}^2 \text{ s}^{-1}$, grey line, Fig. 8a). The anticyclonic benthic boundary layer reaches to approximately 60 m above the bed (grey line, Fig. 8b). In the cyclonic case the benthic boundary layer is constrained near the bed and does not reach the pycnocline (shown as the height of maximum stratification given by the maximum value of the square of the buoyancy frequency, $N^2 = -\frac{g}{\rho_0} \frac{\partial \rho}{\partial z}$). The height of N^2 here is controlled by the surface boundary layer, set by wind and waves and seen in the region of high K_z near the surface. Where tidal currents are anticyclonic, the benthic boundary layer reaches to the pycnocline (yellow N^2 line, Fig. 8b), consistent with Soulsby (1983) which explained that in anticyclonic tidal currents the benthic boundary layer thickness is often limited by water depth or stratification. At the two sites similar surface forcing causes a similar surface boundary layer, but the small height of the cyclonic boundary layer allows for quiescent (low turbulence) over a larger fraction of the water column than in the anticyclonic case, where the surface boundary layer and benthic boundary layer are only separated by approximately 20 m.

The cyclonic location in the model corresponds to the location of site A in a Celtic Sea study, and the anticyclonic location corresponds to site I in the same study, with locations shown on Fig. 3b. In this study, the benthic sediment at site A was characterized as sandy mud ($d_{50} = 57.30 \pm 25.70 \text{ } \mu\text{m}$) and at site I was characterized as muddy sand ($d_{50} = 121.51 \pm 30.33 \text{ } \mu\text{m}$) (Thompson et al., 2017a). The strength of the tidal currents at the two locations was similar.

5. Discussion

5.1. Effects of limited benthic boundary layer thickness on fine sediment

The benthic boundary layer of limited thickness will influence the presence of fine particles in two ways: by promoting deposition and aiding retention. Particles are maintained in suspension by the balance of vertical turbulence and particle settling (O'Brien, 1933; Rouse, 1937). Given the same water column height and surface forcing (i.e. wind and wave surface boundary layer), a larger portion of the water column with cyclonic tidal current rotation has low turbulence, upsetting any equilibrium between settling and turbulence, and thus favoring deposition. The second mechanism is the limit on vertical excursion of resuspended material. Particles eroded and resuspended are not likely to move vertically above the benthic boundary layer because above the boundary layer they will find insufficient turbulence to remain in

suspension, thus trapping fine particles in the benthic boundary layer. Conversely, if the benthic boundary layer is large, particles can move farther up into the water column where currents are larger and more likely to transport fine particles across or off the continental shelf, e.g., to 60 m above the bed versus 20 m above the bed in the water column shown in Fig. 8.

The cyclonic $e = 0.86$ virtual mooring is located within the Celtic Sea mud patch described in Section 4.1.3, and corresponds to a site investigated as part of a seasonal and spatial study of benthic biogeochemistry (Thompson et al., 2017a). In situ erosion experiments and short-term velocity measurements showed that the muddy bed at this location is highly erodible across seasons, and bed shear stresses from tidal currents are often above the critical erosion threshold (Thompson et al., 2017b). Furthermore, trawling of the *N. norvegicus* grounds disturbs the bed, preventing consolidation of the mud deposit (Thompson et al., 2017a). Similar trawling impacts have also been documented in the Irish Sea mud deposits (Coughlan et al., 2015). The limited boundary layer here acts to trap these resuspended muds – whether resuspended by currents, waves, or anthropogenic means. Farther west in the Celtic Sea, where Ward et al. (2015) predicted the presence of fine sediment in the lower bed shear stress environment, the tidal current ellipticity becomes slightly negative. Without the limiting rotational influence, the benthic boundary layer here occupies a larger fraction of the water column suggesting that fine particles are less likely to settle and those on the bed if resuspended may move higher in the water column where the possibility of transport is more likely.

5.2. Benthic boundary layer thickness as a control on mud deposits

To look at the shelf-wide benthic boundary layer reduction and its relationship to mud deposits, we plot the normalized boundary layer thickness, δ^* given by Eq. (11) for the entire shelf (Fig. 9). This formulation developed from the analytical model of Prandle (1982) includes the effects of ellipticity, currents, and depth. The benthic boundary layer thickness predictor does not give all of the dynamical information provided by numerical modeling of K_z over the water column (Fig. 8), but allows us to focus specifically on the combined effects of currents, depth, and ellipticity. Values of $\delta^* > 1$ have been set to 1, and in these regions tidal currents are sufficient to create a benthic boundary layer that covers the entire water column. Where $\delta^* < 1$, a combination of u , H , and e limit the boundary layer thickness. Small δ^* is seen in the Aran Grounds, Celtic Sea, northern Irish Sea, and northern

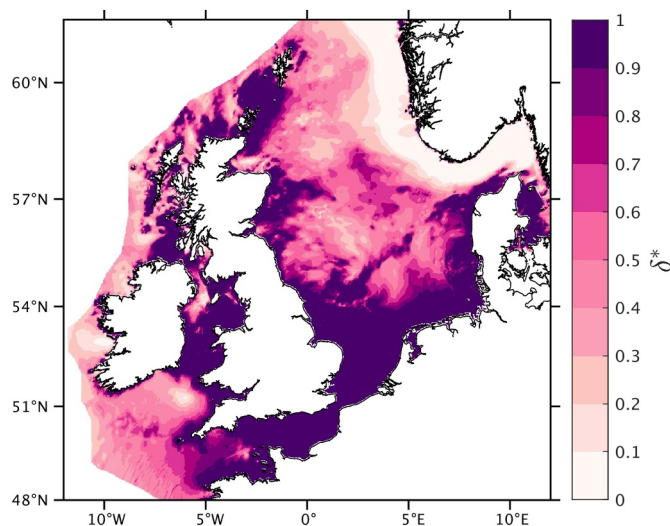


Fig. 9. The ratio of tidal boundary layer thickness to water depth over the Northwest European shelf using the rotational δ_R prediction by Soulsby (1983). Where δ^* is less than one, tidal currents (including ellipticity effects) are insufficient to form a benthic boundary layer covering the entire water column.

North Sea, as well as near the Scottish coast and in the Norwegian trench (Fig. 9). The spatial structure of δ^* agrees well with the spatial distribution of mud deposits on the shelf (Fig. 10), highlighting that mud deposits exist at locations with thin benthic boundary layers. Based on the approximations of c and C_D (Section 2), the Aran Grounds mud deposit exists where the benthic boundary layer is $\leq 10\%$ of the water column (Fig. 10a). In the Aran Grounds, muds as well as bio-fouled microplastics are retained in the sea floor (Martin et al., 2017). The deposition and retention mechanism for negatively buoyant bio-fouled microplastics will be similar to that of sediment, suggesting the influence of the limited boundary layer may extend beyond trapping of muds. The spatial distribution of the eastern Irish sea mud matches nearly perfectly the δ^* contours, and good agreement is seen in the western Irish Sea (Fig. 10b). In the eastern Irish Sea, Ward et al. (2015) over-predicted sediment sizes, but adding the boundary layer effects of cyclonic tidal current rotation could explain this discrepancy through an additional physical mechanism limiting transport of fine particles. Radioactive sediments from nuclear facilities at Sellafield confirm that the region is depositional for locally sourced material (Kershaw et al., 1988). In the western Irish Sea, Fig. 10b shows a reduced boundary layer from the combined influence of depth-averaged tidal currents, ellipticity, and depth. The importance of the seasonal stratified gyre here (e.g. Hill et al., 1996, 1994) alongside the other influencing factors is difficult to quantify. In the Celtic Sea, the tidal boundary layer is limited to 10–20% of the water column (Fig. 10c). Similar to the western Irish Sea, a stratified gyre there may also be of secondary

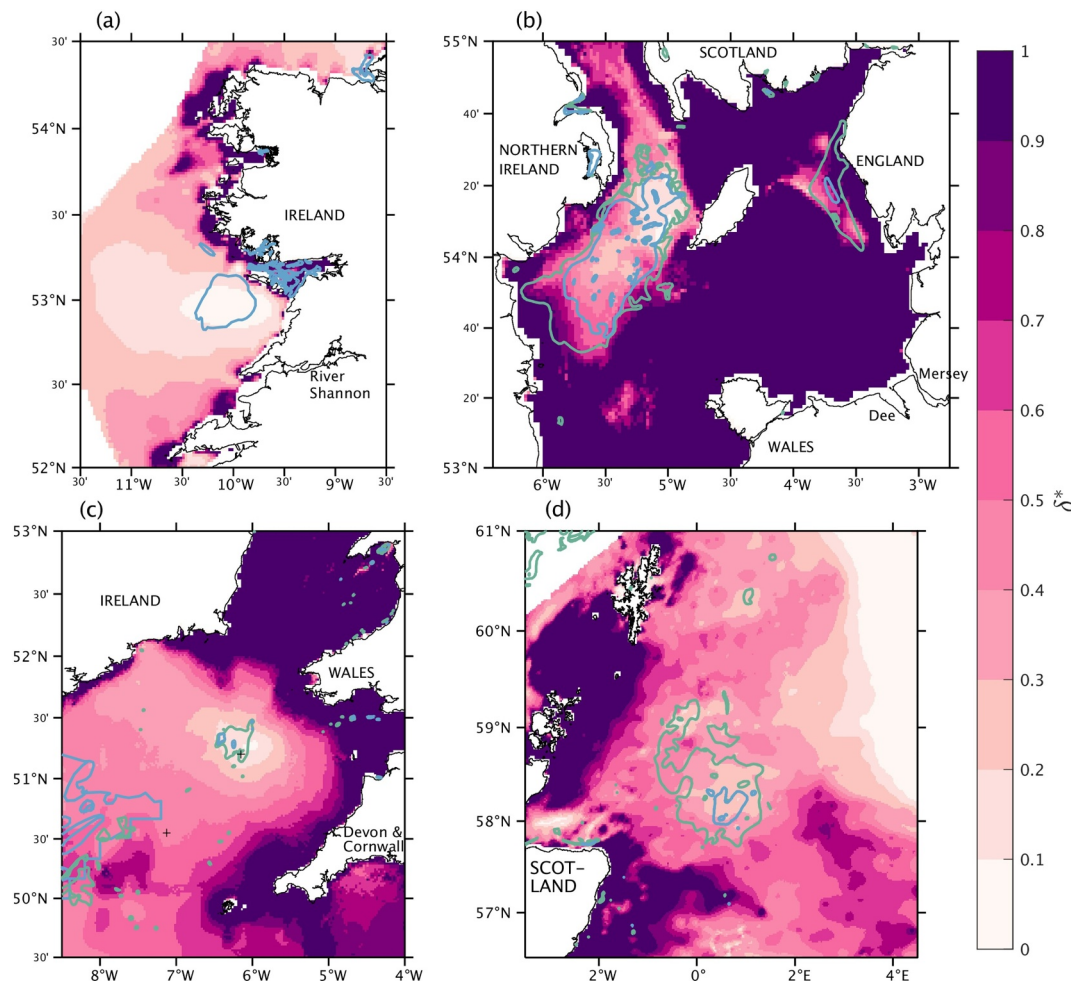


Fig. 10. The ratio of tidal boundary layer thickness to water depth in four regions in the Northwest European shelf. Sediments from the mud corner of the Folk 15 triangle are outlined in green while high mud percentage ($M + (g)M$) sediment is outlined in blue. (a) West of Ireland, (b) the northern Irish Sea, (c) the Celtic Sea, and (d) the northern North Sea. (For interpretation of the references to color in this figure legend, the reader is referred to the web version of this article.)

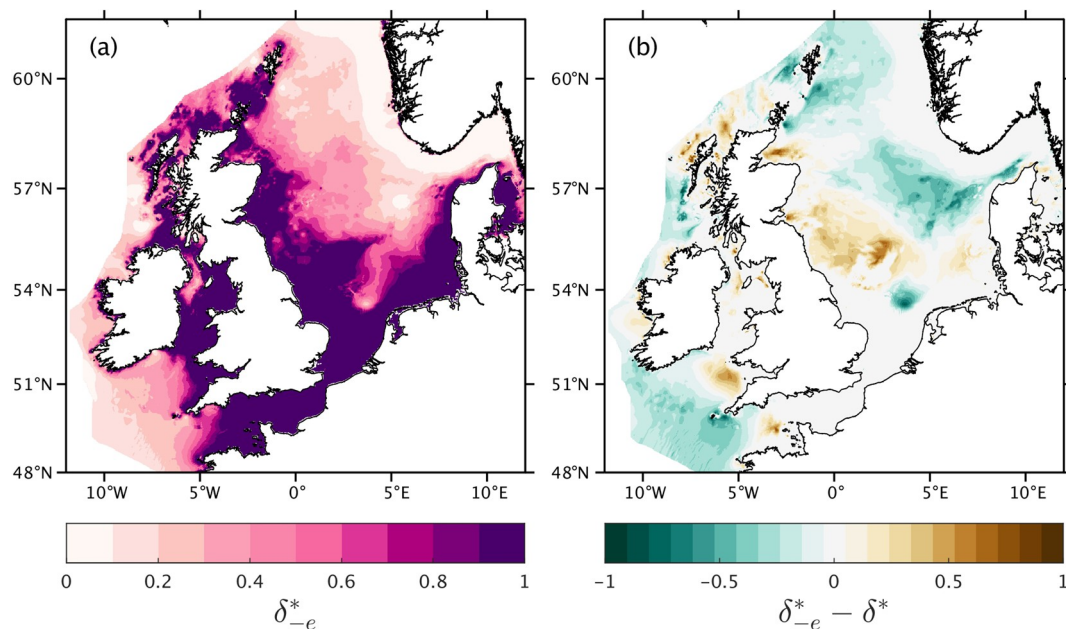


Fig. 11. (a) The scaled benthic boundary layer thickness calculated with ellipticity of the opposite sign to the calculated M_2 ellipticity. (b) The difference between the opposite ellipticity δ_{-e}^* and the real ellipticity δ^* shown in Fig. 9. Brown regions see the boundary layer grow from the real case while blue-green regions see it shrink. (For interpretation of the references to color in this figure legend, the reader is referred to the web version of this article.)

importance to mud retention (Brown et al., 2003). In the northern North Sea, δ^* is also smaller where muds are present (Fig. 10d).

5.3. Ellipticity influence on suppressed benthic boundary layer

The formulation of δ^* in Eq. (11) includes depth and velocity in addition to ellipticity, so to understand the importance of e in this calculation, the sign on the M_2 ellipticity was reversed (δ_{-e}^* , Fig. 9). The spatial structure of the limited boundary layer changes where ellipticity is limiting the boundary layer. The difference between the reversed δ_{-e}^* and accurate δ^* ellipticity cases shows an increased boundary layer in several regions in the Northwest European shelf seas (brown, Fig. 11b). In these locations, tidal ellipticity is a factor in the benthic boundary layer thickness. Where no change occurs ($\delta_{-e}^* - \delta^* \approx 0$), the equation predicts that depth and/or tidal currents control the boundary layer thickness. These values represent both areas where tidal currents are strong enough to fully mix the water column regardless of the sign on the ellipticity as well as locations where deep waters or slow tidal currents do not allow a thick boundary layer to form. These include the Norwegian trench where δ^* is mostly less than 0.1 in both cases and the English Channel where δ^* remains equal to one (Figs. 9, 11a). Locations in blue-green (negative $\delta_{-e}^* - \delta^*$) would have a thinner benthic boundary layer if ellipticity were reversed. These regions correspond to those with strongly anticyclonic tidal currents (Fig. 3b).

Outlining the mud deposits on the four focus regions of the Northwest European shelf seas identifies which locations are most likely influence by ellipticity (Fig. 12). Within the Aran Grounds, the eastern Irish Sea, and the Celtic Sea, the predicted boundary layer thickness would increase if ellipticity were reversed (Fig. 12a–c). The eastern Irish Sea deposit in particular would have a large increase in the boundary layer with reversed ellipticity, and the spatial distribution of this change is in good agreement with the mud deposit outline. In the western Irish Sea, the eastern edge of the mud patch would see a thicker boundary layer with reversed ellipticity, suggesting that the spatial structure of ellipticity influences the spatial structure of the mud deposit there, though over much of the deposit other factors (depth or tidal currents) control the boundary layer thickness as predicted here. In the northern North Sea, ellipticity looks to play a minimal part in the predicted reduced benthic boundary layer, as the outline of the deposit

corresponds to a value of $\delta_{-e}^* - \delta^*$ close to zero (Fig. 12d).

5.4. Relevance compared to other mechanisms of mud deposition and retention

Recent work has shown that episodic events are capable of transporting large quantities of fine sediment. These events include storm induced wave-enhanced sediment-gravity flows (WESGF), resuspension by internal waves, and resuspension by trawling, all coupled with a transport mechanism for these resuspended sediments (Zhang et al., 2016; Cheriton et al., 2014; Payo-Payo et al., 2017). Storm effects to redistribute muddy sediment on the Iberian shelf have been observed and modeled as a combination of WESGF with storm-induced currents, providing a high concentration region and a residual flow to create a large sediment flux (Zhang et al., 2016). These episodic WESGF are seen to be persistent in sediment records (Macquaker et al., 2010). Internal wave has also been seen to suspend muddy sediment on the Monterey Bay shelf edge in the US state of California, providing a mechanism for muds transported off the shelf to move landward through suspended nephroid layers (Cheriton et al., 2014). On the Spanish and French shelves of the Mediterranean Sea, trawling suspends sediment on the shelf edge, and where this occurs proximate to steep canyons, a sediment-gravity flow can be induced to create a large offshore flux of fine sediment (Payo-Payo et al., 2017). These mechanisms are varied, but all exhibit an episodic nature. The mechanism of fine sediment deposition and retention described in this paper is likely to be small on a short-term (hours to days or timescale of episodic events) basis compared to these other episodic events shown to redistribute fine sediment. However, the process described is persistent, so if a large redistribution of sediment by storms occurs only infrequently, a smaller but continuous background of enhanced sediment deposition where the benthic boundary layer is thin may still have a similar impact on a shelf deposit. Measurements of suspended sediment concentrations, along with settling velocities and residual currents would be needed over the full tidal boundary layer to quantify the sediment flux in regions of limited benthic boundary layer, whether the process of boundary layer suppression is by ellipticity or another factor. Conversely, interaction between storm conditions and thin benthic boundary layers may be the mechanism that releases fine sediment from these regions. Storm winds

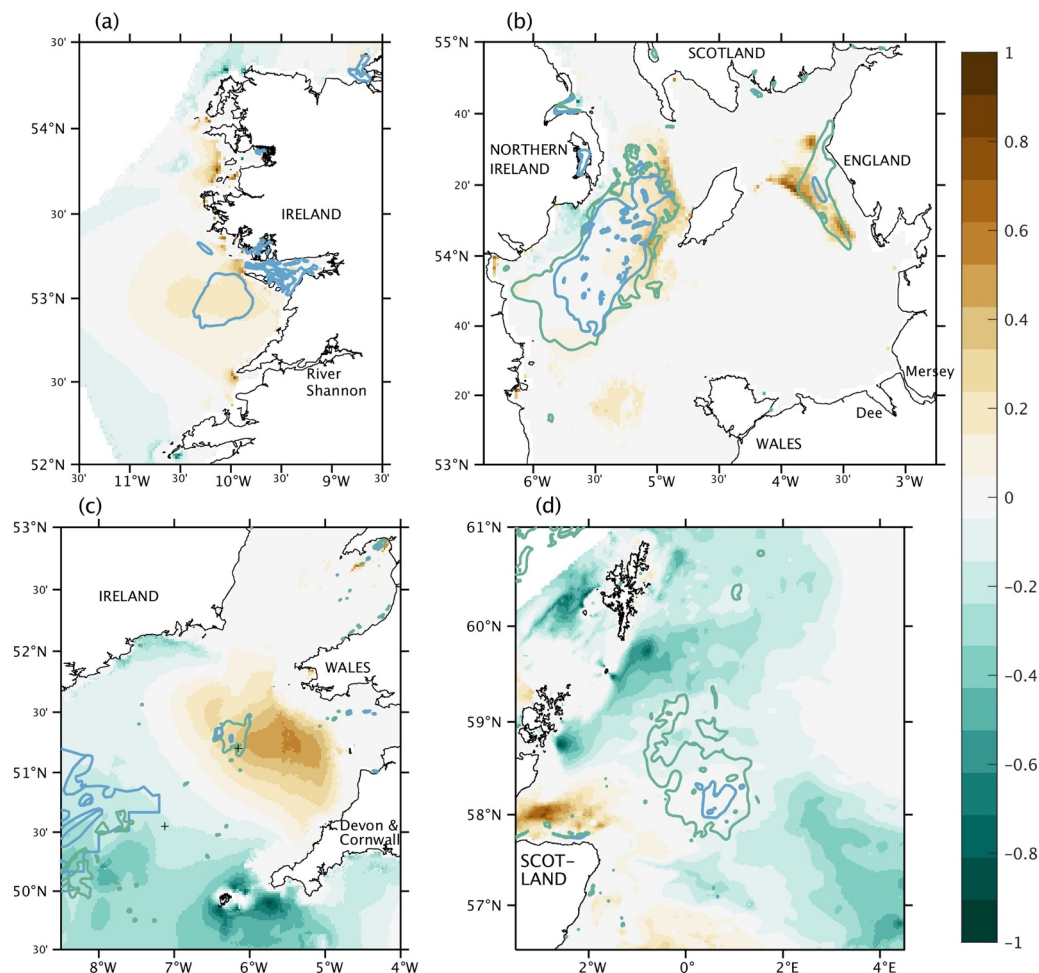


Fig. 12. The difference between the opposite ellipticity δ^*_e and the real ellipticity δ^e shown in Fig. 9 for four focused regions of the Northwest European shelf seas with the mud corner of the Folk 15 triangle outlined in green and high mud percentage (M + (g)M) sediment outlined in blue to show the location of mud deposits. (a) West of Ireland, (b) the northern Irish Sea, (c) the Celtic Sea, and (d) the northern North Sea. (For interpretation of the references to color in this figure legend, the reader is referred to the web version of this article.)

can cause a surface boundary layer that reaches the benthic boundary layer (or the bed in shallow water/very strong winds). In these conditions the mechanisms for retention in regions of cyclonic tidal currents would no longer be retentive - potentially providing an escape path for materials trapped under calm conditions.

Spatially, the episodic processes to distribute muds all occur near the shelf edge. There, high energy from internal waves or surface waves is likely to be greater than on the middle of a large shelf. Transport of trawled sediment in the Mediterranean relied on canyons to act as a conduit to move fine sediment from the shelf edge to deeper regions (Payo-Payo et al., 2017), and internal waves on the Monterey Bay shelf were resuspending fine sediment that had already been transported over the shelf edge (Cheriton et al., 2014). The Northwest European shelf seas are a low energy environment compared to these shelf edges and others with frequently studied mud deposits (e.g. the Eel River shelf and the Waipaoa River shelf, Puig et al., 2003; Hale et al., 2014; Moriarty et al., 2015). Away from the shelf edge, high energy events are less likely, and the importance of limited tidal benthic boundary layer mechanisms on fine sediment deposition and retention may be of greater importance. If this is the case the mechanism described here may be most important in other large shelf seas where mud deposits are found, such as the Yellow and Bohai Seas and the Patagonian shelf (Zhou et al., 2015; Lantzsich et al., 2014).

6. Conclusions

Comparing sediment composition maps and a hydrodynamic numerical model, we have shown here that in the Northwest European shelf seas, fine benthic sediments occur in locations with cyclonic tidal ellipticity. We have suggested that the physical control on this relationship is the influence tidal current rotation has on limiting the thickness of the tidal benthic boundary layer. Using a boundary layer thickness predictor, spatial agreement between mud deposits and limited tidal benthic boundary layer thickness was shown to exist in the Northwest European shelf seas.

This work has shown that a relationship exists between muddy benthic sediment and cyclonic tidal currents in the Northwest European shelf seas. Cyclonic tidal currents, rotating opposite the direction of the Coriolis force, form a smaller tidal benthic boundary layer than anticyclonic currents. This creates a mechanism for enhanced deposition of fine sediment as a greater fraction of the water column has low turbulence above the thin benthic boundary layer and fine material can settle. Once on the sea floor, the thin benthic boundary layer can also limit the movement of resuspended sediment which should be vertically limited by the boundary layer thickness and unable to reach larger residual currents higher in the water column. This mechanism is persistent, though future work is necessary to quantify the resulting sediment fluxes and relate it to other mechanisms of fine sediment dispersion on continental shelf seas.

Data availability

Sediment data are available through the Marine Institute (data.gov.ie/dataset/collated-seabed-substrate) and British Geological Survey (available at emodnet.eu). Model data are available at channelcoast.org/iCOASST.

Acknowledgments

This work was supported by the UK Natural Environment Research Council: Shelf Seas Biogeochemistry NE/K001744/1, NE/K001698/1, and NE/K001906/1, BLUEcoast NE/N015894/1, and iCoast NE/J005444/1. K. Olsen contributed to model processing scripts.

References

- Amoudry, L.O., Souza, A.J., 2011. Deterministic coastal morphological and sediment transport modeling: a review and discussion. *Rev. Geophys.* 49, RG2002. <https://doi.org/10.1029/2010RG000341>.
- Bell, M., Tuck, I., Dobby, H., 2013. *Nephrops* Species. Chapter 12. Wiley-Blackwell, pp. 357–413. <https://doi.org/10.1002/9781118517444.ch12>.
- Bell, M.J., Forbes, R.M., Hines, A., 2000. Assessment of the foam global data assimilation system for real-time operational ocean forecasting. *J. Mar. Syst.* 25, 1–22. [https://doi.org/10.1016/S0924-7963\(00\)00005-1](https://doi.org/10.1016/S0924-7963(00)00005-1).
- Bockelmann, F.-D., Puls, W., Kleeberg, U., Müller, D., Emeis, K.-C., 2018. Mapping mud content and median grain-size of North Sea sediments – a geostatistical approach. *Mar. Geol.* 397, 60–71. <https://doi.org/10.1016/j.margeo.2017.11.003>.
- Boegman, L., Stastna, M., 2019. Sediment resuspension and transport by internal solitary waves. *Annu. Rev. Fluid Mech.* 51, 129–154. <https://doi.org/10.1146/annurev-fluid-122316-045049>.
- Brown, J., Carrillo, L., Fernand, L., Horsburgh, K.J., Hill, A.E., Young, E.F., Medler, K.J., 2003. Observations of the physical structure and seasonal jet-like circulation of the Celtic Sea and St. George's Channel of the Irish Sea. *Cont. Shelf Res.* 23, 533–561. [https://doi.org/10.1016/S0278-4343\(03\)00008-6](https://doi.org/10.1016/S0278-4343(03)00008-6).
- Brown, J.M., Amoudry, L.O., Souza, A.J., Plater, A.J., 2015a. Residual circulation modelled at the national UK scale to identify sediment pathways to inform coastal evolution models. In: Wang, P., Rosati, J.D., Cheng, J. (Eds.), *The Proceedings of the Coastal Sediments 2015*. World Scientific. https://doi.org/10.1142/9789814689977_0137.
- Brown, J.M., Amoudry, L.O., Souza, A.J., Rees, J., 2015b. Fate and pathways of dredged estuarine sediment spoil in response to variable sediment size and baroclinic coastal circulation. *J. Environ. Manag.* 149, 209–221. <https://doi.org/10.1016/j.jenvman.2014.10.017>.
- Brown, J.M., Norman, D.L., Amoudry, L.O., Souza, A.J., 2016. Impact of operational model nesting approaches and inherent errors for coastal simulations. *Ocean Model.* 107, 48–63. <https://doi.org/10.1016/j.ocemod.2016.10.005>.
- Cheriton, O.M., McPhee-Shaw, E.E., Shaw, W.J., Stanton, T.P., Bellingham, J.G., Storlazzi, C.D., 2014. Suspended particulate layers and internal waves over the southern Monterey Bay continental shelf: an important control on shelf mud belts? *J. Geophys. Res.* 119, 428–444. <https://doi.org/10.1002/2013JC009360>.
- Clark, P.U., Mix, A.C., 2002. Ice sheets and sea level of the Last Glacial Maximum. *Quat. Sci. Rev.* 21, 1–7. [https://doi.org/10.1016/S0277-3791\(01\)00118-4](https://doi.org/10.1016/S0277-3791(01)00118-4).
- Costanza, R., d'Arge, R., de Groot, R., Farber, S., Grasso, M., Hannon, B., Limburg, K., Naeem, S., O'Neill, R.V., Paruelo, J., Raskin, R.G., Sutton, P., van den Belt, M., 1997. The value of the world's ecosystem services and natural capital. *Nature* 387, 253. <https://doi.org/10.1038/387253a0>.
- Coughlan, M., Wheeler, A.J., Dorschel, B., Lordan, C., Boer, W., Gaever, P., de Haas, H., Mörz, T., 2015. Record of anthropogenic impact on the Western Irish Sea mud belt. *Anthropocene* 9, 56–69. <https://doi.org/10.1016/j.ancene.2015.06.001>.
- Cullen, P., McCarthy, T.K., 2003. Hydrometric and meteorological factors affecting the seaward migration of silver eels (*Anguilla anguilla*, L.) in the lower River Shannon. *Environ. Biol. Fish.* 67, 349–357. <https://doi.org/10.1023/A:1025878830457>.
- Davies, A., 1985. On determining current profiles in oscillatory flows. *Appl. Math. Model.* 9, 419–428. [https://doi.org/10.1016/0307-904X\(85\)90107-6](https://doi.org/10.1016/0307-904X(85)90107-6).
- Defant, A., 1961. *Physical Oceanography*. 2. Pergamon Press, Oxford, pp. 598.
- Folk, R.L., 1954. The distinction between grain size and mineral composition in sedimentary-rock nomenclature. *J. Geol.* 62, 344–359.
- Fréchette, M., Butman, C.A., Geyer, W.R., 1989. The importance of boundary-layer flows in supplying phytoplankton to the benthic suspension feeder, *Mytilus edulis* L. *Limnol. Oceanogr.* 34, 19–36. <https://doi.org/10.4319/lo.1989.34.1.0019>.
- Grant, W.D., Madsen, O.S., 1986. The continental-shelf bottom boundary layer. *Annu. Rev. Fluid Mech.* 18, 265–305. <https://doi.org/10.1146/annurev.fl.18.010186.001405>.
- Hale, R., Ogston, A., Walsh, J., Orpin, A., 2014. Sediment transport and event deposition on the Waipaoa River Shelf, New Zealand. *Cont. Shelf Res.* 86, 52–65. <https://doi.org/10.1016/j.csr.2014.01.009>.
- Harris, C.K., Wiberg, P.L., 1997. Approaches to quantifying long-term continental shelf sediment transport with an example from the Northern California STRESS mid-shelf site. *Cont. Shelf Res.* 17 (11), 1389–1418. [https://doi.org/10.1016/S0278-4343\(97\)00017-4](https://doi.org/10.1016/S0278-4343(97)00017-4).
- Hill, A.E., Brown, J., Fernand, L., 1996. The western Irish Sea gyre: a retention system for Norway lobster (*Nephrops norvegicus*)? *Oceanol. Acta* 19, 357–368.
- Hill, A.E., Durazo, R., Smeed, D.A., 1994. Observations of a cyclonic gyre in the western Irish Sea. *Cont. Shelf Res.* 14, 479–490. [https://doi.org/10.1016/0278-4343\(94\)90099-X](https://doi.org/10.1016/0278-4343(94)90099-X).
- Holt, J., Proctor, R., 2008. The seasonal circulation and volume transport on the north-west European continental shelf: a fine-resolution model study. *J. Geophys. Res.* 113. <https://doi.org/10.1029/2006JC004034>.
- Holt, J., Umlauf, L., 2008. Modelling the tidal mixing fronts and seasonal stratification of the Northwest European Continental shelf. *Cont. Shelf Res.* 28, 887–903. <https://doi.org/10.1016/j.csr.2008.01.012>.
- Holt, J.T., Allen, J.I., Proctor, R., Gilbert, F., 2005. Error quantification of a high-resolution coupled hydrodynamic-ecosystem coastal-ocean model: part 1 model overview and assessment of the hydrodynamics. *J. Mar. Syst.* 57, 167–188. <https://doi.org/10.1016/j.jmarsys.2005.04.008>.
- Holt, J.T., James, I.D., 2001. An s coordinate density evolving model of the northwest European continental shelf: 1. Model description and density structure. *J. Geophys. Res.* 106, 14015–14034. <https://doi.org/10.1029/2000JC000304>.
- Hsiao, S.V., Shemdin, O.H., 1980. Interaction of ocean waves with a soft bottom. *J. Phys. Oceanogr.* 10, 605–610. [https://doi.org/10.1175/1520-0485\(1980\)010<0605:IOOWWA>2.0.CO;2](https://doi.org/10.1175/1520-0485(1980)010<0605:IOOWWA>2.0.CO;2).
- Jansen, J.H.F., 1976. Late Pleistocene and Holocene history of the northern North Sea, based on acoustic reflection records. *Neth. J. Sea Res.* 10, 1–43. [https://doi.org/10.1016/0077-7579\(76\)90002-8](https://doi.org/10.1016/0077-7579(76)90002-8).
- Jansen, J.H.F., Doppert, J.W.C., Hoogendoorn-Toering, K., de Jong, J., Spaik, G., 1979. Late Pleistocene and Holocene deposits in the Witch and Fladen Ground area, Northern North Sea. *Neth. J. Sea Res.* 13, 1–39. [https://doi.org/10.1016/0077-7579\(79\)90031-0](https://doi.org/10.1016/0077-7579(79)90031-0).
- Jørgensen, B.B., 1983. The major biogeochemical cycles and their interactions. In: Bolin, B., Cook, R.B. (Eds.), *SCOPE* 21. Wiley, New York, pp. 477–509.
- Kershaw, P.J., Swift, D.J., Denoon, D.C., 1988. Evidence of recent sedimentation in the eastern Irish Sea. *Mar. Geol.* 85, 1–14. [https://doi.org/10.1016/0025-3227\(88\)90081-3](https://doi.org/10.1016/0025-3227(88)90081-3).
- Komen, G.J., Cavaleri, L., Donelan, M., Hasselmann, K., Hasselmann, S., Janssen, P.A.E.M., 1994. *Dynamics and Modelling of Ocean Waves*. Cambridge University Press. <https://doi.org/10.1017/CBO9780511628955>.
- Lantzsch, H., Hanebuth, T.J., Chiessi, C.M., Schwenk, T., Violante, R.A., 2014. The high-supply, current-dominated continental margin of southeastern South America during the late Quaternary. *Quat. Res.* 81, 339–354. <https://doi.org/10.1016/j.yqres.2014.01.003>.
- Lorke, A., Müller, B., Maerki, M., Wüest, A., 2003. Breathing sediments: the control of diffusive transport across the sediment-water interface by periodic boundary-layer turbulence. *Limnol. Oceanogr.* 48, 2077–2085. <https://doi.org/10.4319/lo.2003.48.6.2077>.
- Macquaker, J.H., Bentley, S.J., Bohacs, K.M., 2010. Wave-enhanced sediment-gravity flows and mud dispersal across continental shelves: reappraising sediment transport processes operating in ancient mudstone successions. *Geology* 38, 947. <https://doi.org/10.1130/G31093.1>.
- Martin, J., Lusher, A., Thompson, R.C., Morley, A., 2017. The deposition and accumulation of microplastics in marine sediments and bottom water from the Irish continental shelf. *Sci. Rep.* 7, 10772. <https://doi.org/10.1038/s41598-017-11079-2>.
- McCave, I.N., 1972. Transport and escape of fine-grained sediment from shelf areas. In: Swift, D.J.P., Duane, D.B., Pilkey, O.H. (Eds.), *Shelf Sediment Transport: Process and Pattern*. Dowden, Hutchinson and Ross, Stroudsburg, pp. 225–244.
- Monbaliu, J., Padilla-Hernández, R., Hargreaves, J.C., Albiach, J.C.C., Luo, W., Scialvo, M., Günther, H., 2000. The spectral wave model, WAM, adapted for applications with high spatial resolution. *Coast. Eng.* 41, 41–62. [https://doi.org/10.1016/S0378-3839\(00\)00026-0](https://doi.org/10.1016/S0378-3839(00)00026-0).
- Moriarty, J.M., Harris, C.K., Hadfield, M.G., 2015. Event-to-seasonal sediment dispersal on the Waipaoa River Shelf, New Zealand: a numerical modeling study. *Cont. Shelf Res.* 110, 108–123. <https://doi.org/10.1016/j.csr.2015.10.005>.
- Neill, S.P., Scourse, J.D., Uehara, K., 2010. Oct. Evolution of bed shear stress distribution over the northwest European shelf seas during the last 12,000 years. *Ocean Dyn.* 60, 1139–1156. <https://doi.org/10.1007/s10236-010-0313-3>.
- O'Brien, M.P., 1933. Review of the theory of turbulent flow and its relation to sediment-transportation. *Eos. Trans. AGU* 14, 487–491. <https://doi.org/10.1029/TR014i001p00487>.
- O'Neill, C.K., Polton, J.A., Holt, J.T., O'Dea, E.J., 2012. Modelling temperature and salinity in Liverpool Bay and the Irish Sea: sensitivity to model type and surface forcing. *Ocean Sci.* 8, 903–913. <https://doi.org/10.5194/os-8-903-2012>.
- Pawlowski, R., Beardsley, B., Lentz, S., 2002. Classical tidal harmonic analysis including error estimates in MATLAB using TIDE. *Comput. Geosci.* 28, 929–937. [https://doi.org/10.1016/S0098-3004\(02\)00013-4](https://doi.org/10.1016/S0098-3004(02)00013-4).
- Payo-Payo, M., Jacinto, R., Lastras, G., Rabineau, M., Puig, P., Martín, J., Canals, M., Sultan, N., 2017. Numerical modeling of bottom trawling-induced sediment transport and accumulation in La Fonera submarine canyon, northwestern Mediterranean Sea. *Mar. Geol.* 386, 107–125. <https://doi.org/10.1016/j.margeo.2017.02.015>.
- Pingree, R.D., Griffiths, D.K., 1977. The bottom mixed layer on the continental shelf. *Estuar. Coast. Mar. Sci.* 5, 399–413. [https://doi.org/10.1016/0302-3524\(77\)90064-0](https://doi.org/10.1016/0302-3524(77)90064-0).
- Prandle, D., 1982. The vertical structure of tidal currents and other oscillatory flows. *Cont. Shelf Res.* 1, 191–207. [https://doi.org/10.1016/0278-4343\(82\)90004-8](https://doi.org/10.1016/0278-4343(82)90004-8).
- Puig, P., Ogston, A., Mullenbach, B., Nittrouer, C., Sternberg, R., 2003. Shelf-to-canyon sediment-transport processes on the Eel continental margin (northern California). *Mar. Geol.* 193, 129–149. [https://doi.org/10.1016/S0025-3227\(02\)00641-2](https://doi.org/10.1016/S0025-3227(02)00641-2).
- Rees, H.L., Pendle, M.A., Waldoock, R., Limpenny, D.S., Boyd, S.E., 1999. A comparison of benthic biodiversity in the North Sea, English Channel, and Celtic Seas. *ICES J. Mar.*

- Sci. 56, 228–246. <https://doi.org/10.1006/jmsc.1998.0438>.
- Rouse, H., 1937. Modern conceptions of the mechanics of fluid turbulence. *Trans. Am. Soc. Civ. Eng.* 102, 463–543.
- Sharples, J., Ellis, J.R., Nolan, G., Scott, B.E., 2013. Fishing and the oceanography of a stratified shelf sea. *Prog. Oceanogr.* 117, 130–139. <https://doi.org/10.1016/j.pocean.2013.06.014>.
- Simpson, J.H., Tinker, J.P., 2009. A test of the influence of tidal stream polarity on the structure of turbulent dissipation. *Cont. Shelf Res.* 29, 320–332. <https://doi.org/10.1016/j.csr.2007.05.013>.
- Somerfield, P.J., McClelland, I.L., McNeill, C.L., Bolam, S.G., Widdicombe, S., 2018. Environmental and sediment conditions, infaunal benthic communities and biodiversity in the Celtic Sea. *Cont. Shelf Res.* <https://doi.org/10.1016/j.csr.2018.09.002>.
- Soulsby, R.L., 1983. The bottom boundary layer of shelf seas. In: Johns, B. (Ed.), *Physical Oceanography of Coastal and Shelf Seas*. Elsevier, Amsterdam, pp. 189–266.
- Soulsby, R.L., 1997. *Dynamics of Marine Sands*. Thomas Telford, London.
- Stephens, D., Diesing, M., 2015. Towards quantitative spatial models of seabed sediment composition. *PLoS One* 10, 11. <https://doi.org/10.1371/journal.pone.0142502>.
- Thompson, C.E.L., Silburn, B., Williams, M.E., Hull, T., Sivy, D., Amoudry, L.O., Widdicombe, S., Ingels, J., Carnovale, G., McNeill, C.L., Hale, R., Marchais, C.L., Hicks, N., Smith, H.E.K., Klar, J.K., Hiddink, J.G., Kowalik, J., Kitidis, V., Reynolds, S., Woodward, E.M.S., Tait, K., Homoky, W.B., Kröger, S., Bolam, S., Godbold, J.A., Aldridge, J., Mayor, D.J., Benoist, N.M.A., Bett, B.J., Morris, K.J., Parker, E.R., Ruhl, H.A., Statham, P.J., Solan, M., 2017a. An approach for the identification of exemplar sites for scaling up targeted field observations of benthic biogeochemistry in heterogeneous environments. *Biogeochemistry* 135, 1–34. <https://doi.org/10.1007/s10533-017-0366-1>.
- Thompson, C.E.L., Williams, M.E., Amoudry, L.O., Hull, T., Reynolds, S., Panton, A., Fones, G.R., 2017b. Benthic controls of resuspension in UK shelf seas: implications for resuspension frequency. *Cont. Shelf Res.* <https://doi.org/10.1016/j.csr.2017.12.005>.
- Umlauf, L., Burchard, H., Bolding, K., 2005. General ocean turbulence model: source code documentation. Baltic Sea Research Institute Warnemünde Technical Report. 63. pp. 346.
- van Rijn, L.C., 2007. Unified view of sediment transport by currents and waves. I: initiation of motion, bed roughness, and bed-load transport. *J. Hydraul. Eng.* 133, 649–667. [https://doi.org/10.1061/\(ASCE\)0733-9429\(2007\)133:6\(649\)](https://doi.org/10.1061/(ASCE)0733-9429(2007)133:6(649)).
- Ward, S.L., Neill, S.P., Van Landeghem, K.J.J., Scourse, J.D., 2015. Classifying seabed sediment type using simulated tidal-induced bed shear stress. *Mar. Geol.* 367, 94–104. <https://doi.org/10.1016/j.margeo.2015.05.010>.
- Wilson, R.J., Speirs, D.C., Sabatino, A., Heath, M.R., 2018. A synthetic map of the north-west European Shelf sedimentary environment for applications in marine science. *Earth Syst. Sci. Data* 10, 109–130. <https://doi.org/10.5194/essd-10-109-2018>.
- Winterwerp, J.C., van Kesteren, W.G.M., 2004. *Introduction to the Physics of Cohesive Sediment Dynamics in the Marine Environment*. Elsevier, Amsterdam.
- Zhang, W., Cui, Y., Santos, A.I., Hanebuth, T.J.J., 2016. Storm-driven bottom sediment transport on a high-energy narrow shelf (NW Iberia) and development of mud depocenters. *J. Geophys. Res. Oceans* 121, 5751–5772. <https://doi.org/10.1002/2015JC011526>.
- Zhou, C., Dong, P., Li, G., 2015. Hydrodynamic processes and their impacts on the mud deposit in the Southern Yellow Sea. *Mar. Geol.* 360, 1–16. <https://doi.org/10.1016/j.margeo.2014.11.012>.